Annals of Biomedical Engineering, Vol. 9, pp. 145-164, 1981 0090-6964/81/020145-20 $02.00/0

THEORETICAL ANALYSIS OF ARTERIAL HEMODYNAMICS INCLUDING THE INFLUENCE OF BIFURCATIONS

Part I: Mathematical Model and Prediction of Normal Pulse Patterns

J.C. Stettler*
P. Niederer
and
M. Anliker

Institute of Biomedical Engineering
University of Zurich
and
Swiss Federal Institute of Technology
Zurich, Switzerland

Based on earlier theoretical studies, a new mathematical model is developed for the prediction of the pressure and flow pulses propagating in the arterial system. This model permits a more realistic simulation of bifurcation and stenoses than was possible previously. By making use of a computer, it allows us to calculate the pulse shapes along branching arteries. It is based on the assumption that each arterial conduit can be represented by a suitable combination of three basic segments, namely segments with no or only small-calibre side branches, short segments with big side branches, and short segments with pathological changes of the conduit. Along segments of the first type, the pulse propagation is calculated with the aid of the method of characteristics and a first order integration. For the other two types, the linearized mass balance and momentum equations are utilized together with the boundary conditions to determine the pressure and flow values at the ends of the segment. A standard case for the human arterial conduit extending from the heart to the foot, with eight major branches, is defined using published data and prescribing the ejection pattern from the heart. The computed pulse shapes and their changes with propagation exhibit the characteristic features observed in man under normal conditions.

*Present address: Department of Mechanical Engineering, University of Houston, Houston, Texas 77004. This work was supported in part by Grant 3.121.-0.77 from the Swiss National Science Foundation. Address correspondence to Max Anliker, Institute of Biomedical Engineering, University of Zurich and Swiss Federal Institute of Technology, Moussonstrasse 18, CH-8044 Zurich, Zurich, Switzerland.

1. INTRODUCTION

The pressure and flow pulses generated by the intermittent ejection of blood from the left ventricle of the heart undergo chracteristic nonlinear shape changes as they propagate along the different branches of the arterial tree. These changes are primarily due to the geometrical arrangement and the taper of the arteries as well as the mechanical properties of the vessel wall and the blood. Accordingly, disease or ageing of the arterial conduits may noticeably influence the propagation characteristics of the pulses. Our mathematical analysis of the circulatory system is aimed at providing a better understanding of these phenomena as well as making it possible to predict new features associated with pulse propagation in arteries which had not been recognized or recorded so far.

Advanced ultrasonic Doppler equipment allows us to measure velocity profiles even in arteries that are located in relatively remote positions in the body and which were therefore not accessible to this technique in the past. For example, a new 128 channel ultrasound Doppler velocity meter (1, 14) permits the determination of instantaneous velocity profiles and the flow patterns in vessels within a range of 10 cm, e.g., the abdominal aorta. To facilitate a detailed understanding of the measurements and to reduce the need for empirical data a mathematical model should realistically simulate the arterial system. In particular, it should permit the analysis of the pressure and flow patterns along any arterial conduit extending from the heart to any location of interest in the body and should take into account the influence of side branches. Yet, in view of the limitations of present computing capabilities, such a model can be devised only by introducing reasonable approximations, such as the assumption of one-dimensional flow.

In some of the earlier models (3, 10, 20, 22), the presence of discrete side branches at various locations in an arterial conduit was simulated by a suitably chosen leakage of the arterial wall which varied appropriately with pressure, flow, and distance from the heart. In part, satisfactory results were obtained with these models. However, from an anatomical and mechanical point of view, they are not sufficiently good approximations of reality. Moreover, they lead to numerical instabilities if one attempts to adjust the permeability of the vessel wall to strong local variations as would be the case in areas of major bifurcations or stenoses. In order to better approximate the pertinent features of the arterial tree in normal as well as in pathological situations, the arterial tree is divided into segments which are individually modelled in terms of standardized elements representing tapered tubes, bifurcation regions, and pathological sections, respectively. The tube elements are considered as long compared to the bifurcation regions and as having only small side branches. The feasibility of this approach will be assessed by a comparison of the predicted flow patterns in healthy and pathological cases with US Doppler measurements.

The blood is treated as an incompressible Newtonian fluid and the flow as one-dimensional. This implies that only spatial averages of the pressure and

velocity at a given cross section are calculated. Furthermore, the vessel walls are assumed to be elastic and the cross section of the vessels circular. Small curvatures of the blood vessels are neglected. The numerical solution utilized for the long tube segments is based on the method of characteristics whereby specified time intervals are used.

One-dimensional models with discrete branches have also been analysed by other authors. However, they limited their studies to less general configurations than those aimed at in this paper.

For example, Clark and Kufahl (9) considered the canine brain perfusion while Raines *et al.* (19) investigated the pulse propagation in the human leg. A model for the systemic arterial pulse wave transmission using simplified idealized branch conditions was presented by Schaaf and Abbrecht (23). They disregarded the pressure drop as well as the vessel distensibility in branching structures. We found that this approximation causes a deterioration of the agreement between predicted and measured flow patterns. Finally, a two-dimensional model of the flow through diseased coronary arteries was presented by Back *et al.* (5).

The one-dimensional model of pressure and flow pulse transmission derived from the physical approximations first described by Streeter *et al.* (25) may lead to the formation of shock waves under certain conditions (11, 21). This phenomenon is usually not taken into account in the numerical treatment of such models because no true shock transitions have been observed in the mammalian circulation. However, in patients with a severe aortic insufficiency, the so-called pistol-shot phenomenon can be interpreted as a shocklike wave (3). An examination of the pattern formed by the characteristic curves in our simulations shows that adjacent characteristics originating from the heart during early systole converge at a distance of approximately 50–70 cm. Mathematically, this behavior is typical of shock formation. In a computer solution based on the method of characteristics using specified time intervals, however, this fact is of no consequence because infinitely steep wave fronts are impeded by numerical damping. In the present work this effect was not investigated in detail because in our model the peaks of the distal pulses are inaccurate due to the neglect of vessel wall viscoelasticity. It is to be expected that in the mathematical model shock formation is prevented if this damping effect is properly taken into account (13). Therefore, a comprehensive analysis of shock formation should be undertaken only if the model includes viscoelastic damping mechanisms.

2. MATHEMATICAL MODEL OF THE ARTERIAL SYSTEM

2.1. Geometrical Approximations

The anatomical features of arterial conduits suggest that a mathematical model be synthesized on the basis of different types of elements:

– segments with none or only insignificant side branches;

– bifurcation regions;
– segments with pathological features.

Each of these elements requires different fluid-dynamic approximations which will be described in the following.

2.1.1. Segments with none or only insignificant side branches. We consider a one-dimensional flow situation in a long circular tube with a tapered cross section $S(p(z,t),z)$, whereby z denotes the axial coordinate, which is usually identical with the distance from the heart, t the time and $p(z,t)$ the pressure. The spatially averaged flow velocity is given by $v(z,t)$ (Fig. 1a). The flow of blood through small side branches is taken into account by including a continuous outflow function $\psi(p,v,z)$ simulating a pressure and flow dependent seepage. Based on these approximations, the mass balance and one-dimensional equation for a Newtonian fluid yield (25)

$$\frac{\partial S}{\partial p}\frac{\partial p}{\partial z}v+\frac{\partial S}{\partial z}v+S\frac{\partial v}{\partial z}+\psi+\frac{\partial S}{\partial p}\frac{\partial p}{\partial t}=0 \tag{2.1}$$

$$\frac{\partial}{\partial z}(\rho Sv^2)+\frac{\partial}{\partial t}(\rho Sv)+\rho\psi v=-S\frac{\partial p}{\partial z}+f\ , \tag{2.2}$$

with ρ denoting the density of the blood and f an approximate expression for the friction force due to blood viscosity. As was pointed out by Hughes and Lubliner (15), the continuous outflow occurs in the mass balance equation as well as in the momentum equation. Stettler (24) has shown that the influence of the blood viscosity μ giving rise to the friction term f is only of relevance in arteries with a diameter of less than approximately 1 mm. In such vessels a parabolic velocity profile is predominant (28, 29), such that f may be approximated by

$$f=-8\pi\mu v\ . \tag{2.3}$$

The choice of an explicit form for ψ is deferred to paragraph 2.2.

2.1.2. Bifurcation segments. Whenever a large vessel branches off from the conduit of interest, we define a bifurcation region as shown in Fig. 1b. Its form is approximated by a truncated cone with height h and surfaces S_1 and S_2. For the volume V_B of the bifurcation region the mass balance requires

$$v_1S_1=v_2S_2+v_3S_3+\frac{\mathrm{d}}{\mathrm{d}t}\left(\frac{h}{3}\left[S_1+S_2+\sqrt{S_1S_2}\right]\right)\ . \tag{2.4}$$

In formulating the momentum equation between the points z_1 and $z_j (j=2,3)$ we make use of a modified Bernoulli relation

$$p_1-p_j=\frac{\rho}{2}(v_j^2-v_1^2)+\rho\int_{z_1}^{z_j}\frac{\partial v}{\partial t}\,\mathrm{d}s+\Delta p_j \tag{2.5}$$

in which Δp_j incorporates the pressure loss due to viscous friction of the blood as well as the influence of curvature of the vessels in an approximate fashion. Since individual bifurcations are short compared to the segments described in 2.1.1, the application of the integrated form of the momentum Eq. 2.5 appears to be justified. An empirical expression for Δp_j was given by Prandtl (18) and is based on a quasistationary laminar flow with a spatial mean velocity v in a rigid curved circular tube with a cross-sectional radius R_j and radius of curvature r_j (Fig. 1c). This expression is given by

$$\Delta p_j = \lambda_j \frac{L}{4R_j} v_1^2 \quad , \tag{2.6}$$

where

$$\lambda_j = 0.37 \left(\frac{1}{2} Re_j \cdot \sqrt{\frac{R_j}{r_j}} \right)^{0.36} \cdot \frac{64}{Re_j} \quad \text{for } Re_j \cdot \sqrt{\frac{R_j}{r_j}} \geqslant 10^{1.6}$$

$$= \frac{64}{Re_j} \quad \text{for } Re_j \cdot \sqrt{\frac{R_j}{r_j}} \leqslant 10^{1.6}$$

and

$$Re_j = 2R_j \rho v_1 / \mu \quad .$$

2.1.3. Pathological segments. An important example of a pathological alteration of an arterial segment is a short stenosis (Fig. 2) which has the form of an abrupt and short narrowing of the blood vessel. The length L of the stenosis is less than the computational axial increment Δz defined in paragraph 3. This type of stenosis represents a relatively frequent malformation [e.g., Bollinger (7)] and is accompanied by fat and calcium depositions in the arterial wall which result in a local stiffening of the wall material. We therefore neglect the cross-sectional change with pressure of the entire segment in formulating the mass balance equation between z_1 and z_2 (Fig. 2):

$$v_1 S_1 = v_2 S_2 \quad . \tag{2.7}$$

For the pressure drop $p_1 - p_2$ across the stenosis, an equation similar to Eq. 2.5 can be derived:

$$p_1 - p_2 = \frac{\rho}{2} (v_2^2 - v_1^2) + \rho \int_{z_1}^{z_2} \frac{\partial v}{\partial t} \Delta z + \Delta p \quad . \tag{2.8}$$

Flow separation in points A and B (Fig. 2) is equivalent to an additional narrowing of the cross section. Hence, the stenosis has an effective area S_E. Furthermore, flow separation in C causes an increased pressure drop which is taken into account by using the relation for the so-called Borda–Carnot effect [e.g., Bennett and Myres (6)].

Accordingly we have

$$\Delta p = \underbrace{\frac{\rho}{2} v_1^2 \left(\frac{S_1}{S_E} - 1 \right)^2}_{\text{Borda–Carnot effect}} + \underbrace{8\pi\mu L v_1 S_1 / S_E^2}_{\text{friction between } B \text{ and } C} \tag{2.9}$$

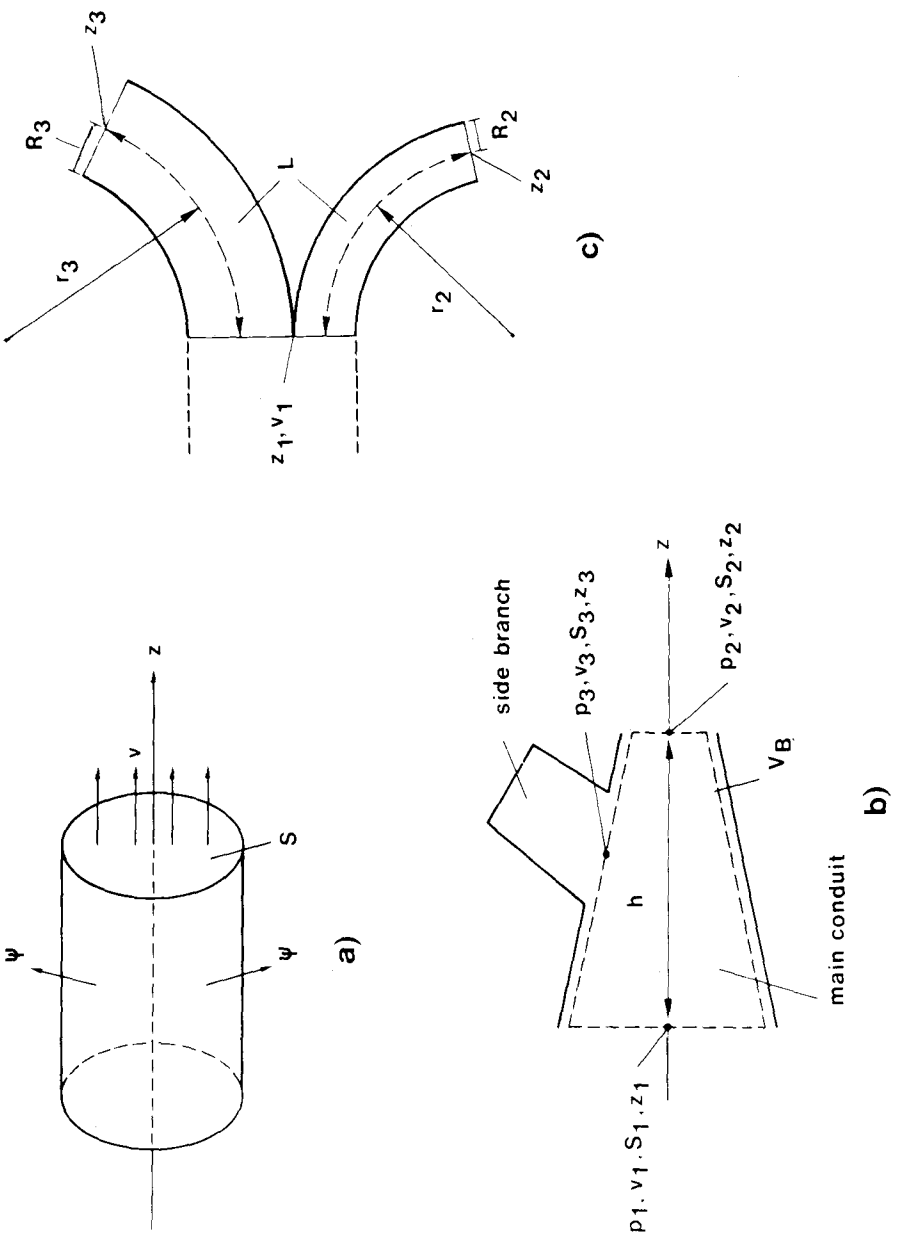

FIGURE 1. Models of arterial elements, from which a conduit is formed: (a) segment with continuous outflow (only small side branches); (b) bifucation segment; (c) geometrical approximations of the branching of the flow in a bifucation.

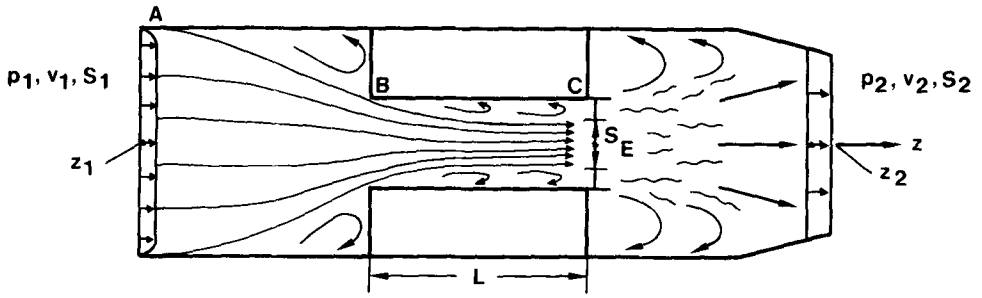

FIGURE 2. Model of a short stenosis.

2.2. Mechanical Aspects

2.2.1. Distensibility of the arterial vessel wall. Anliker *et al.* (3) introduced the vessel wall distensibility in their model by means of prescribing the propagation velocity $c(p,z)$ of small artificially induced pressure perturbations as a function of the pressure and the distance from the heart. In contrast to the elastic constants of the vessel wall material this velocity can be measured under physiological conditions (2) and is related to the wall distensibility $\partial S/\partial p$ by

$$c^2(p,z) = S(p,z) / (\rho \frac{\partial S}{\partial p}) \ . \tag{2.10}$$

As this procedure proved to be advantageous also from a numerical point of view it is adopted in our model. The available results of wave speed measurements indicate that a relation of the form

$$c(p,z) = (c_0 + B \cdot p) \cdot g(z) \tag{2.11}$$

can be used. The two constants c_0 and B as well as the function $g(z)$ are chosen according to the measurements. At present, our knowledge of vessel elasticity under physiological conditions could not support a more refined choice of $c(p,z)$. Upon integrating Eq. 2.10, one obtains for the pressure dependence of $S(p,z)$

$$S(p,z) = S_0(z) \cdot \exp\left[\frac{p - p_0}{c(p_0,z) \cdot \rho \cdot c(p,z)}\right], \tag{2.12}$$

where $S_0(z)$ denotes the cross sectional area at distance z and reference pressure p_0. The vessel described in such a way acts in a purely elastic fashion. The damping of the pulses due to vessel wall viscoelasticity is thereby disregarded. The consequences of this approximation are discussed in paragraph 5.

2.2.2. Outflow conditions. In the case of a parent artery branching into two or more smaller vessels the distribution of blood flow in the individual branches depends on the geometry of the bifurcation as well as the mechanical wall properties. In the long segments described in paragraph 2.1.1 emanating from the heart or a bifurcation, the method of characteristics will be utilized to integrate the pulse propagation equations. Consequent application of this procedure for all first and higher order side branches would however result in a computer program which could no longer be applied efficiently. Therefore, it is desirable to replace side branches of minor interest by suitably chosen lumped outflow resistance elements, which relate the pressure p_3 and flow Q_3 (Fig. 1b) at the entrance of a branch to the pressure p_1 and flow Q_1 in the main conduit.

An outflow condition is derived on the basis of the following heuristic considerations:

- In case of a relatively small rigid branch originating from the main conduit, the outflow through this branch is proportional to

$$Q_3 \sim (p_1 - p_c)S_3^2 \quad .$$

  This relation is derived from the Hagen–Poiseuille law, according to which the (laminar) flow in a rigid tube is proportional to the pressure difference $p_1 - p_c$ (p_c denotes the capillary pressure at the end of the tube) as well as the square of the cross section. The main conduit is thereby regarded as a large reservoir such that the above relation may be assumed independent of the *flow* Q_1.
- In case of a main conduit branching symmetrically into two equal vessels the outflow condition

$$Q_2 = Q_3 = Q_1/2$$

  results from continuity. This relation is independent of the *pressure* p_1.

In general, the flow in the side branch will depend on Q_1 as well as p_1. We therefore combine the two relations given above by stipulating

$$Q_3 = R_p(p_1 - p_c)S_3^2 + R_q Q_1 \quad ; \tag{2.13}$$

R_p and R_q are lumped parameters which have to be chosen appropriately. The relation (Eq. 2.13) cannot be mathematically derived from fluid dynamic laws. Its applicability is shown by direct comparison of results obtained with the method of characteristics and relation (Eq. 2.13), respectively (Part II).

The values of the outflow parameters R_p and R_q are found by means of multilinear regression analysis. First, the side branch under consideration is calculated with the method of characteristics and the resulting values of Q_1, Q_3, S_3, and p_1 are sampled at different times t_j ($j = 1 \ldots N$) during the heart cycle. Then, these values are introduced in Eq. 2.13 such that a set of N linear equations results for R_p and R_q.

Considerations similar to those given above are applied to obtain an expression for the continuous outflow function $\psi(p,z)$ introduced in Eq. 2.1,

$$\psi(p,z) = \phi_p(z)(p - p_c)S^2 + \phi_q(z) \cdot S \cdot v \ . \tag{2.14}$$

In this relation $\phi_p(z)$ and $\phi_q(z)$ serve as outflow parameters. The choice of these functions is given in paragraph 4.

3. NUMERICAL SOLUTION

3.1 Application of the Method of Characteristics

Equations 2.1 and 2.2 which govern the pulse propagation along segments with none or only insignificant side branches form a system of quasilinear hyperbolic partial differential equations. The numerical solution is found by utilizing the method of characteristics and specified time intervals. Since in our model the bifurcations are treated separately, the functions $S_0(z)$ and $\psi(p,z)$ exhibit only a relatively weak dependence of z. Therefore, a first order integration scheme is applicable (10).

Upon transforming the system Eqs. 2.1, 2.2 and using Eq. 2.3 the two characteristic directions

$$\frac{dz}{dt} = v \pm c \tag{3.1}$$

are obtained, whereby c is given by Eq. 2.10. The characteristic equations are

$$dv \pm \frac{dp}{\rho c} = \left(-\frac{8\pi\mu v}{\rho s} \mp \frac{vc}{S}\frac{\partial S}{\partial z} \mp \frac{c}{S}\psi\right) dt \ . \tag{3.2}$$

For the solution to be numerically stable the Courant stability criterion [e.g., Lister (16)] for the step sizes Δz and Δt

$$\frac{\Delta z}{\Delta t} \geqq |v| + c \tag{3.3}$$

has to be fulfilled for all integration points z_j and time steps t_j.

3.2. Boundary Conditions

We consider an arbitrary arterial system which is built up from two segment types mentioned in paragraph 2.1 (Fig. 3). While the coordinate z applies to the main conduit, i.e., the conduit in which we want to study the pulse propagation, at each bifurcation a new axial coordinate z_{B_n} for the nth side branch originating at that location has to be defined. Each branch and each segment may have their own spatial and temporal step sizes Δz_{B_n} and Δt_{B_n}.

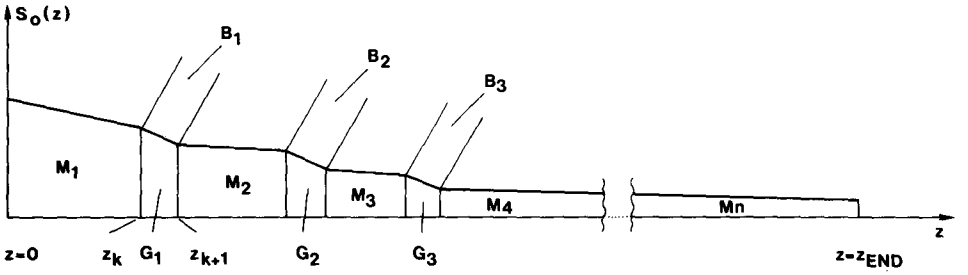

FIGURE 3. Principle of subdividing an arterial conduit into long segments M_i, bifurcations G_i, and side branches B_i.

In order that a unique solution for the characteristic Eqs. 3.2 exists, a complete set of boundary conditions has to be specified. At the root of the aorta ($z = 0$ in the main conduit) we prescribe the ejection pattern of the left ventricle in the form of the volume flow rate $Q_0(t)$, whereby the shape of the curve is assumed to be equal to the one given by Wetterer and Kenner (27). At the distal end of the main conduit and of each side branch which is not replaced by outflow parameters either a constant capillary pressure p_c, a constant venous pressure, or a peripheral resistance is given. The boundary conditions used for all segments ending or originating in a bifurcation are described for the bifurcation shown in Fig. 4. We assume the velocities and pressures at the boundary of the bifurcation volume at time t_0 to be known, namely $v(z_n)$ and $p(z_n)$, $v(z_n + \Delta z)$, and $p(z_n + \Delta z)$, as well as $v(z_{B_n} = 0)$ and $p(z_{B_n} = 0)$. If we restrict ourselves to the simple case $\Delta t_{B_n} = \Delta t$, the six unknowns, namely velocities and pressures at the boundaries of the bifurcation volume at time $t_0 + \Delta t$, are calculated with the aid of the following six relations:

- the characteristic Eqs. 3.2 along the characteristic directions C_1 and C_2 in the main conduit,
- either the characteristic equation along the characteristic direction C_3 in the z_{B_n}, t_{B_n} plane of the side branch, or the outflow condition (Eq. 2.13) in case of replacement of the side branch by outflow parameters,
- mass balance Eq. 2.4 for the bifurcation volume G_n,
- integrated momentum Eq. 2.5 with Eq. 2.6 between points z_n and $z_n + \Delta z$, z_n and $z_{B_n} = 0$, respectively.

In order to make Eqs. 2.5 and 2.6 amenable to numerical solution, the term

$$\rho \int_{z_1}^{z_2} \frac{\partial v}{\partial t} \, dz$$

is approximated by

$$\rho \cdot \frac{\Delta z}{2\Delta t} \left\{ v(z_n, t_0 + \Delta t) + v(z_n + \Delta z, t_0 + \Delta t) - [v(z_n, t_0) + v(z_n + \Delta z, t_0)] \right\}$$

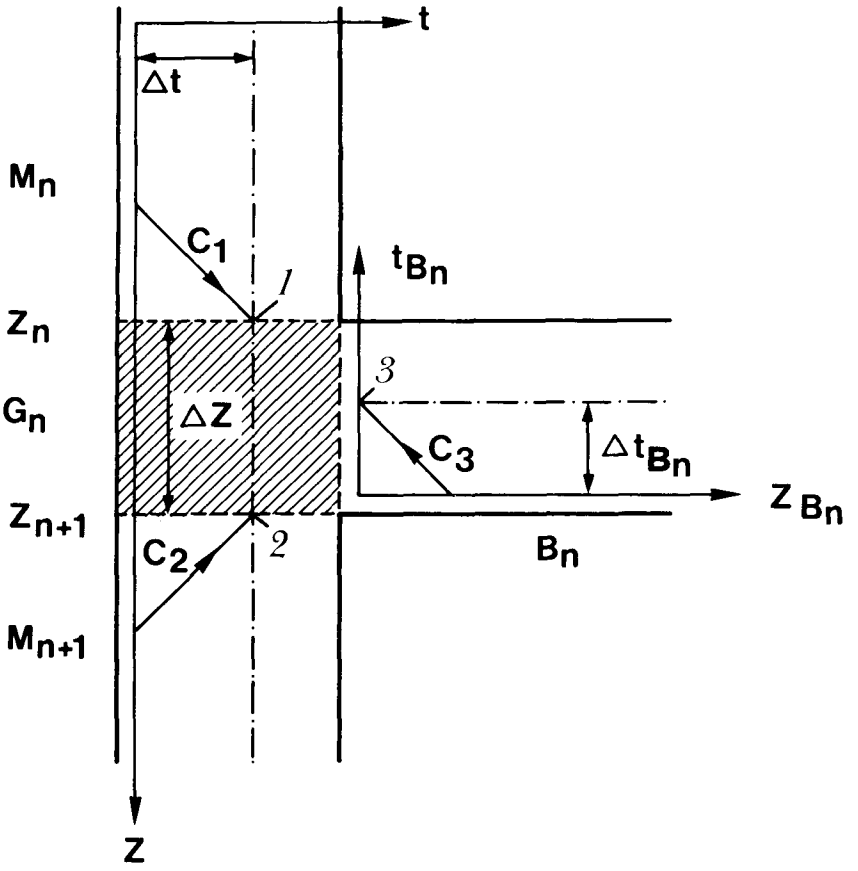

FIGURE 4. Boundary conditions for bifurcation G_n: C_1, C_2, and C_3 denote characteristic directions in the coordinate system z,t (points 1 and 2), and z_{B_n}, t_{B_n} (point 3), respectively.

and the quadratic terms in v are linearized with respect to the increments within the time interval Δt.

In case of unequal integration step size for the adjoining branches interpolation procedures are applied, as described in detail by Stettler (24). The boundary conditions for pathological segments are treated in the same manner as shown for the bifurcations.

4. STANDARD CASE OF HUMAN ARTERIAL TREE

4.1. General Layout

We examine the pulse propagation in a human arterial conduit which extends from the root of the aorta to the foot (Fig. 5). A standard case is defined by choosing the physiological and geometrical quantities such that they correspond to an average healthy human adult on the basis of present

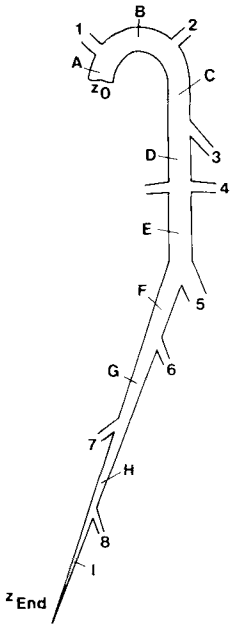

SEGMENT		SIDE BRANCH	
A	A. ASCENDENS	1	CORONAR A., TRUNCUS
B	ARCUS AORTAE		BRACHIOCEPAHLICUS
C	A. THORACALIS	2	A. CAROTIS SINISTRA
D	A. THORACALIS		A. SUBCLAVIA SINISTRA
E	A. ABDOMINALIS	3	TRUNCUS COELIACUS
F	A. ILIACA COM.	4	A. RENALIS
G	A. FEMORALIS	5	BIFURCATION
H	A. FEMORALIS	6	A. ILIACA INTERNA
	A. POPLITEA	7	A. PROFUNDA FEMORALIS
I	A. TIBIALIS ANT.,	8	A. TIBIALIS POST.,
	A. DORSALIS PEDIS		A. PERONAEA

FIGURE 5. Definition of a standard case of an arterial conduit extending from the root of the aorta ($z = 0$) to the foot ($z = 155$ cm) with eight side branches.

knowledge. It consists of a main conduit and eight side branches. The side branches 1, 2, 3, and 6 corresponding to coronary arteries and *truncus brachiocephalicus,* left carotid and subclavian arteries, *truncus coeliacus,* and internal iliac artery, respectively, are replaced by outflow parameters. A detailed analysis of the flow characteristics in these branches, especially in the vessels leading to the head, will be relegated to a future study.

4.2. Distribution of Cross Sections

Based partly on the measurements published by Westerhof *et al.* (26) and partly on our own investigations the coordinates z_{jn} of the discrete branch sites and the values of S at the reference pressure $p_0 = 100$ mm Hg were chosen as schematically indicated in Fig. 6. The side branch 5 is assumed to be identical to the main conduit for $z \geqslant 42.5$ cm, as in a healthy subject the bifurcation of the abdominal aorta into the two iliac arteries is expected to be symmetrical.

4.3. Wave Speed and Blood Parameters

We choose c_0, B, and $g(z = 0)$ of Eq. 2.11 as follows [see also Elsner (10)]:

$$c_0 = 140 \text{ cm/sec}$$
$$B = 2 \text{ cm/(sec} \cdot \text{mm Hg)}$$
$$g(z = 0) = 1.$$

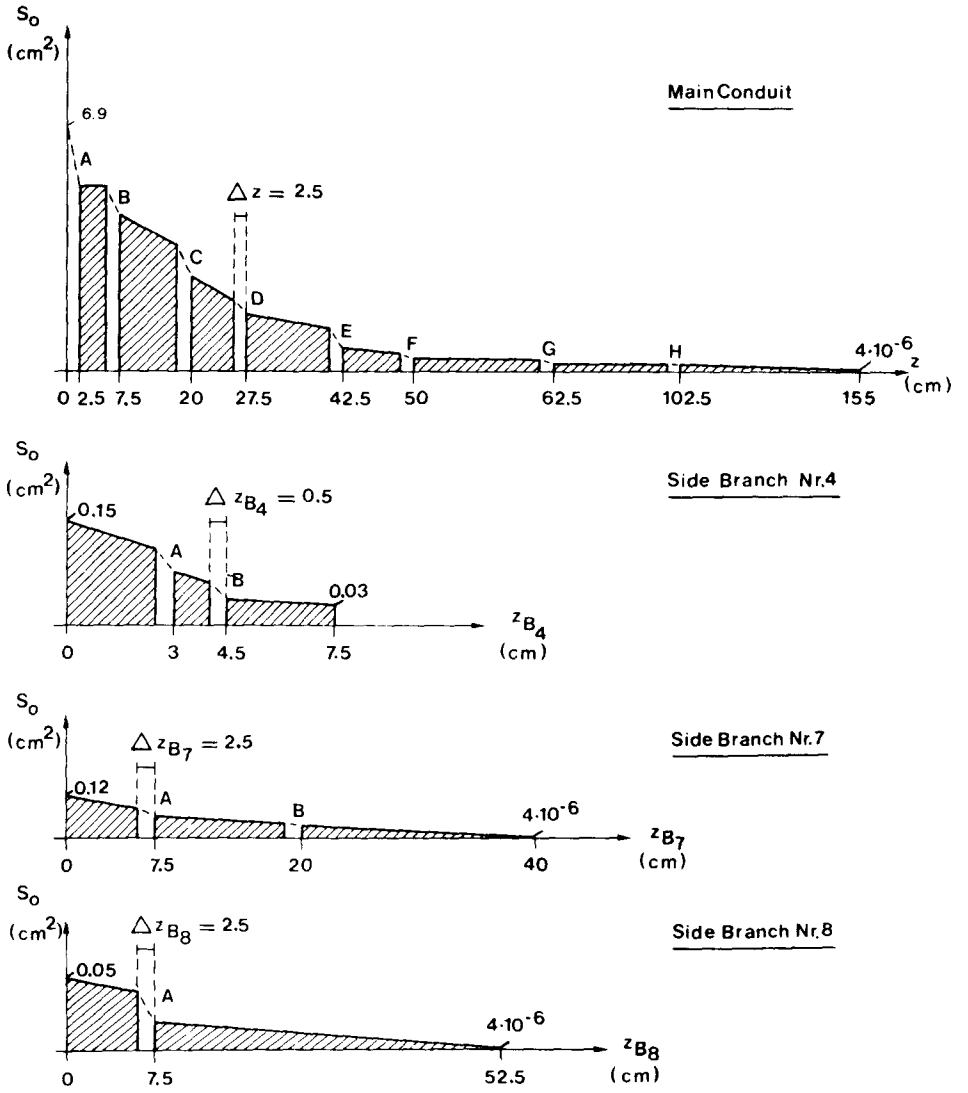

FIGURE 6. Geometrical properties and numerical constants Δz and Δt of standard case. The cross-sections S_1, S_2, S_3 at the bifurcations (cf. Fig. 2) are chosen as follows in (cm²): $\Delta t = \Delta t_{B_7} = \Delta t_{B_8} = 0.002$ sec; $\Delta t_{B_4} = 0.0004$ sec.

Main conduit: bifurcation	*A*	*B*	*C*	*D*	*E*	*F*	*G*	*H*
S_1	6.9	5.5	3.6	2.0	1.3	0.53	0.26	0.09
S_2	5.5	4.5	2.7	1.6	0.7	0.35	0.18	0.05
S_3	1.4	1.0	1.0	0.15	0.7	0.35	0.12	0.05

(Note: In bifurcation *D*, S_3 is the cross-section for one renal artery.)

Side branch 4.: bifurcation	A	B
S_1	0.11	0.06
S_2	0.075	0.035
S_3	0.1	0.05

Side branch 7: bifurcation	A	B
S_1	0.08	0.04
S_2	0.06	0.03
S_3	0.06	0.04

Side branch 8: bifurcation	A
S_1	0.04
S_2	0.02
S_3	0.02

The dependence on z of $c(p,z)$ at the reference pressure $p_0 = 100$ mm Hg is assumed to be linear and the corresponding parameters are given in Table 1. The density of the blood ρ is set equal to 1.06 g/cm^3 and its viscosity $\nu = 0.049$ P.

4.4. *Outflow, Seepage, and Curvature Parameters*

Since in the model presented here the outflow from the long segments is insignificant the actual choice of the seepage parameters $\phi_p(z)$ and $\phi_q(z)$ has little influence on the calculated pulse shapes. We therefore set $\phi_q(z) = 0$ and $\phi_p(z)$ according to Table 2.

The regression method to determine the outflow parameters R_p and

TABLE 1. Dependence on z of $c(p_0,z)$ with $p_0 = 100$ mm Hg.

	z cm	$c(p_0,z)$ cm/sec
Main conduit	0	340
	102.5	800
	155	950
Side branch 4	0	678
	7.5	841
Side branch 7	0	700
	40	950
Side branch 8	0	800
	52.5	950

Between the given values the dependence is assumed linear. Side branch 5 is identical to the main conduit for $z \geqq 42.5$ cm.

TABLE 2. Dependence on z of $\phi_p(z)$ (ml/dyn · sec).

Main conduit	z	$\leqslant 5$ cm	$\leqslant 40$ cm	$\leqslant 100$ cm	$\leqslant 155$ cm
	$\phi_p(z)$	0	10^{-7}	$0.5\ 10^{-8}$	$3.3\ 10^{-7}$
Side branch 4			$\phi_p(z) = 0$		
Side branch 7	z	<20 cm	$\geqslant 20$ cm		
	$\phi_p(z)$	0	$4.5\ 10^{-7}$		
Side branch 8	z	<5 cm	$\geqslant 5$ cm		
	$\phi_p(z)$	0	$3.3\ 10^{-7}$		

Side branch 5 is identical to the main conduit for $z \geqq 42.5$ cm.

R_q described in paragraph 2.2.2 is only applied for branches 4, 5, 7, and 8 in which $p(z,t)$ and $v(z,t)$ have been calculated explicitly by the method of characteristics. Until further flow studies in the side branches 1, 2, 3, and 6 have been performed, their R_p and R_q values have to be found empirically by matching pressure and ultrasonic flow measurements (24). Table 3 shows the chosen values together with the assumed curvature parameters. Since the influence of the pressure drop due to curvature was found to be minimal, this effect is neglected when the method of characteristics is applied to side branches. Table 4 exhibits the outflow parameters for the bifurcations of the side branches 4, 7, and 8.

5. REPRESENTATIVE RESULTS FOR STANDARD CASE

The computed pressure and flow pulses shown in Figs. 7, 8, and 9 exhibit a good overall agreement with published measurements (7, 8, 17, 27). The characteristic features of the arterial pressure and flow pulses as they are ob-

TABLE 3. Outflow and curvature parameters of the 8 discrete bifurcations of the standard case.

Branch No.	R_q	$R_p\ 10^{-6}$ $\left(\frac{\text{cm}}{\text{dyn sec}}\right)$	R_2/r_2	R_3/r_3
1	0.06	150	0.6	0.6
2	0.05	113	0.7	0.7
3	0.0087	274	0.0	0.7
4	0.0023	50	0.0	0.7
5	0.5	0.0	0.1	0.1
6	0.35	13.7	0.1	0.1
7	0.35	6.92	0.1	0.1
8	0.5	0.0	0.1	0.1

TABLE 4. Outflow and curvature parameters for the bifurcations of side branches 4, 7, 8.

Branch No.	Bifurcation No.	R_q	$R_p\ 10^{-6}$ $\left(\frac{\text{cm}}{\text{dyn sec}}\right)$	R_2/r_2	R_3/r_3
4	1	0.5	0	0	0
	2	0.5	0	0	0
7	1	0.0	7	0	0
	2	0.0	28	0	0
8	1	0.5	0	0	0

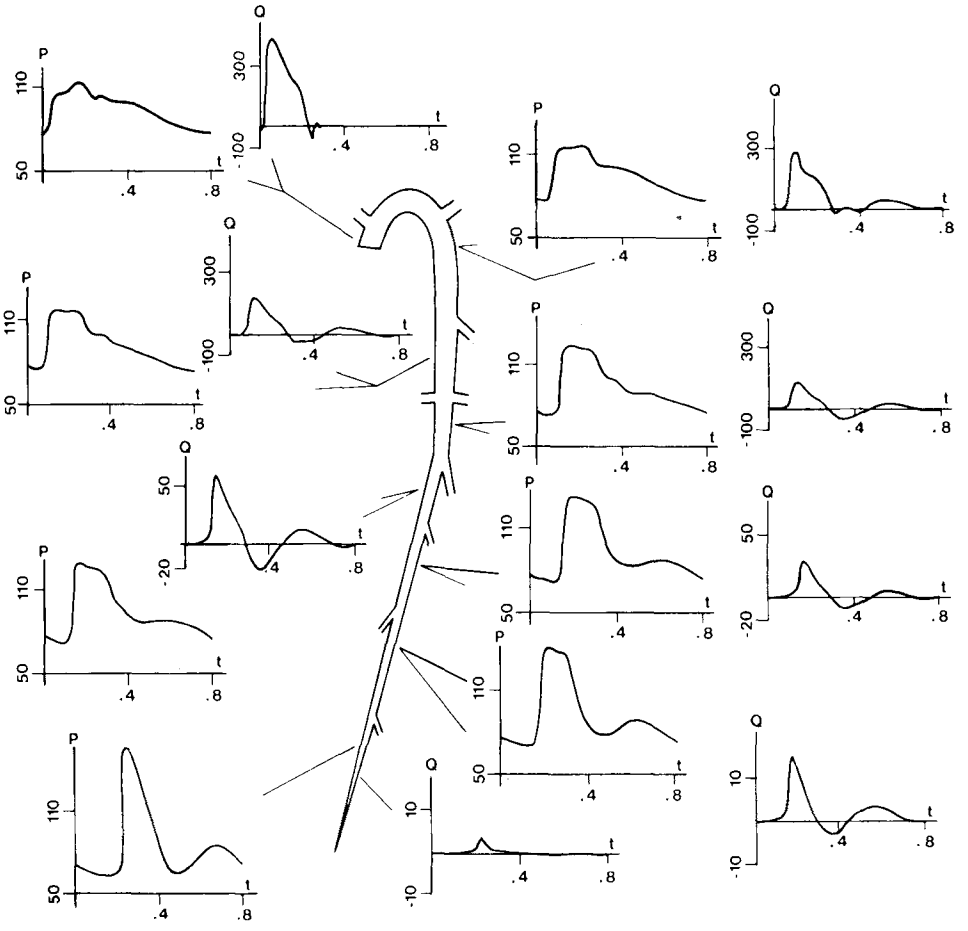

FIGURE 7. Calculated pressures and flow patterns at different locations for standard case. Pressures are given in mm Hg, and flows in ml/sec.

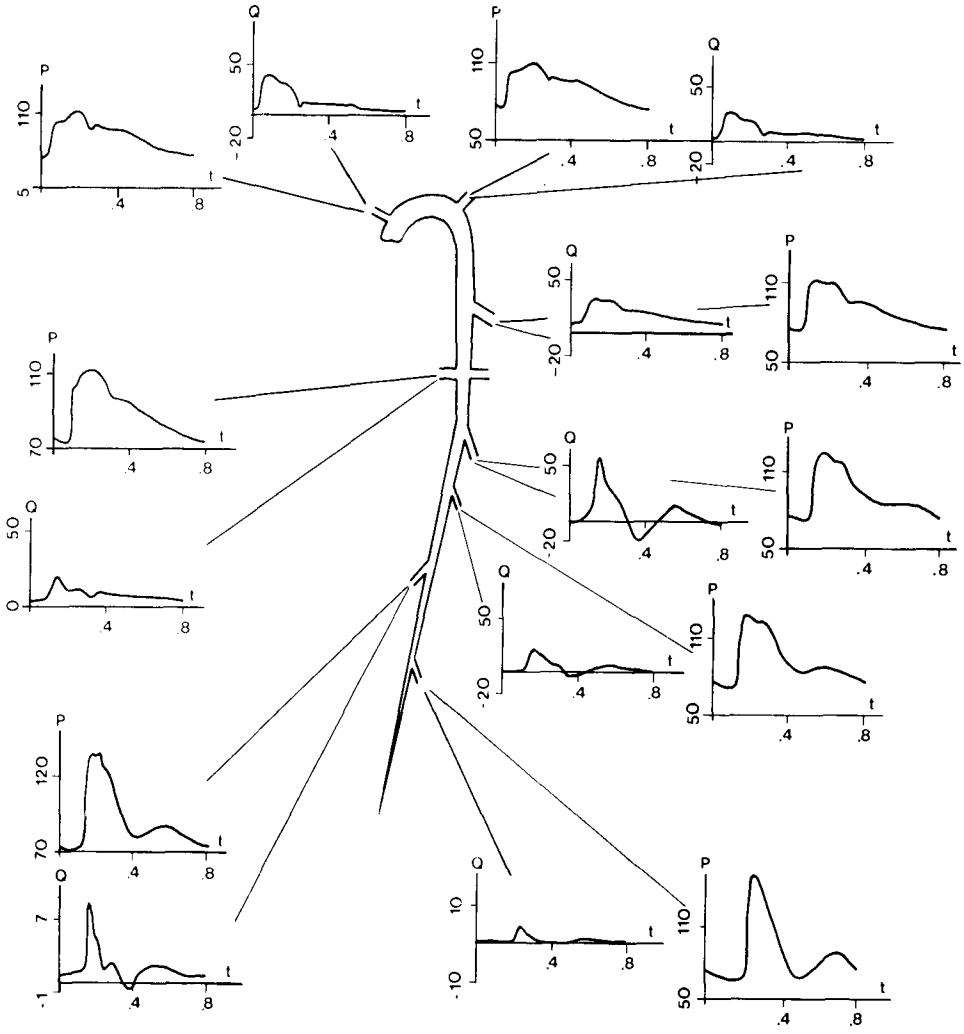

FIGURE 8. Calculated pressures and flow patterns at the entrance of the 8 side branches of standard case. Same units as Fig. 7.

served in man as well as their changes with increasing distance from the heart are clearly reproduced. In particular, the theoretical results document the presence of the incisura up to the bifurcation at $z = 42.5$ cm. Furthermore, they predict a gradual decrease of the diastolic pressure and increase of the systolic pressure with increasing distance from the heart. Besides this, they show a steepening of the wave front up to a distance of about 140 cm. Beyond the bifurcation the development of a dichrotic pressure wave is observed. In addition, the flow pulse shows a progressively pronounced backflow during diastole with increasing distance from the heart until the diameter is reduced to approximately 0.3 cm.

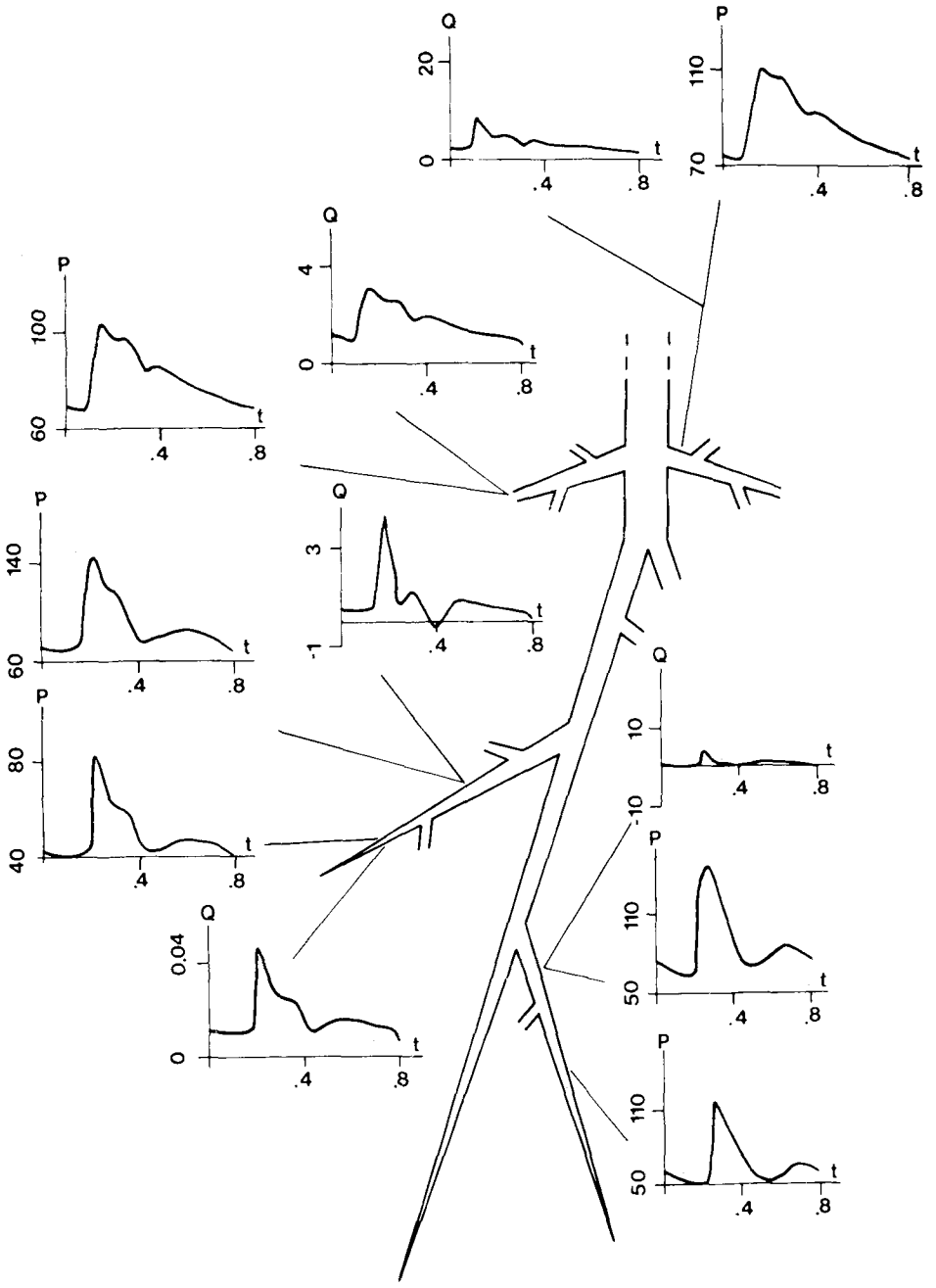

FIGURE 9. Calculated pressures and flow patterns in side branches 4, 5, 7, and 8 of standard case at the indicated locations. Same units as Fig. 7.

However, in the most distal region the calculated flow pulse exhibits a relatively sharp peak, which is not observed in healthy persons. To some extent, this fact can be attributed to the neglect of the vessel wall visco-

elasticity as has been substantiated by Anliker *et al.* (4) and Holenstein *et al.* (12, 13). Furthermore, it has to be noted that also the damping due to blood viscosity is underestimated by the present model [Eq. 2.3, see Zielke (30)]. A more detailed critical evaluation of the mathematical model described here will be given in Part II. Finally, the ultimate utility of the model tested will be revealed for its predictive capabilities in pathological situations.

REFERENCES

1. Anliker, M., M. Casty, P. Friedli, R. Kubli, and H. Keller. Noninvasive measurement of blood flow. In: *Cardiovascular Flow Dynamics and Measurements*, edited by N.H.C. Hwang and N.A. Normann. Baltimore, MD: University Park Press, 1977.
2. Anliker, M., M.B. Histand, and E. Ogden. Dispersion and attenuation of small pressure waves in the canine aorta. *Circ. Res.* 23:539, 1968.
3. Anliker, M., R.L. Rockwell, and E. Ogden. Nonlinear analysis of flow pulses and shock waves in arteries. Part I: Derivation and properties of mathematical model. Part II: Parametric study related to clinical problems. *J. Appl. Math. Phys.* (ZAMP). 22:217–246 (Part I), 563–581 (Part II), 1971.
4. Anliker, M., J.C. Stettler, P. Niederer, and R. Holenstein. Prediction of shape changes of propagating flow and pressure pulses in human arteries. In: *The Arterial System*, edited by R.D. Bauer and R. Busse. Heidelberg: Springer, 1978.
5. Back, L., J. Radbill, and D. Crawford. Analysis of pulsatile, viscous blood flow through diseased coronary arteries of man. *J. Biomech.* 10:339, 1977.
6. Bennett, C.O. and J.E. Myres. *Momentum, Heat and Mass Transfer*, 2nd ed., Chemical Eng. Ser., New York: McGraw-Hill, 1974.
7. Bollinger, A. *Funktionelle Angiologie*. Stuttgart: Thieme, 1979.
8. Casty, M. Perkutane atraumatische Flussmessung in grösseren hautnahen Gefässen mit einem vielkanaligen gepulsten Ultraschall-Dopplergerät. Dissertation. University of Zurich, 1976.
9. Clark, M.E. and R.H. Kufahl. Simulation of the cerebral macrocirculation. In: *Cardiovascular System Dynamics*, edited by J. Baan and A. Noordergraaf. Boston: MIT Press, 1978.
10. Elsner, J. Mathematische Modellstudien der Druck–und Flusspulse in menschlichen Arterien. Dissertation No. 5582. Swiss Federal Institute of Technology, Zurich, Switzerland, 1975.
11. Forbes, L.K. A note on the solution of the one-dimensional unsteady equations of arterial blood flow by the method of characteristics. *J. Aust. Math. Soc.* 21:45–52, 1979.
12. Holenstein, R., P. Niederer, and J.C. Stettler. A structural damping model of arterial viscoelasticity in predicting flow and pressure pulses. In: Conference Digest, 1st International Conference on Mechanics in Medicine and Biology. Baden-Baden: Verlag Gerhard Witzstrock, 1978.
13. Holenstein, R., P. Niederer, and M. Anliker. A viscoelastic model for use in predicting arterial pulse waves. *ASME J. Biomech. Eng.* 102:318–319, 1980.
14. Hübscher, W. and M. Anliker. Instantane Flussmessungen in grossen Blutgefässen mittels 128-kanaligem Ultraschall-Doppler-Gerät und Mikroprozessor. *Medita.* 9a/1977.
15. Hughes, T. and J. Lubliner. On the one-dimensional theory of blood flow in larger vessels. *Math. Biosci.* 18:161, 1973.
16. Lister, M. The numerical solution of hyperbolic differential equations by the method of characteristics. In: *Mathematics for Digital Computers*. New York: J. Wiley & Sons, 1960.
17. McDonald, R. *Blood Flow in Arteries*, 2nd ed. London: Arnold, 1974.
18. Prandtl, L. *Führer durch die Strömungslehre*, 3rd ed. Braunschweig, 1948, p. 159.
19. Raines, J., M. Jaffrin, and A.H. Shapiro. A computer simulation of arterial dynamics in the human leg. *J. Biomech.* 7:77, 1974.
20. Rockwell, R.L., M. Anliker, and J. Elsner. Model studies of the pressure and flow pulses in a viscoelastic arterial conduit. *J. Franklin Inst.* 297:405, 1974.
21. Rudinger, G. Shock waves in mathematical models of the aorta. *J. Appl. Mech.* 37:34, 1970.
22. Rumberger, J.A. and R.M. Nerem. A method-of-characteristic calculation of coronary blood flow. *J. Fluid. Mech.* 182:429, 1977.
23. Schaaf, B.W. and P.H. Abbrecht. Digital computer simulation of human systemic arterial pulse wave transmission: A nonlinear model. *J. Biomech.* 5:345, 1972.

24. Stettler, J.C. Theoretische Untersuchungen der arteriellen Hämodynamik unter Berücksichtigung von Verzweigungen. Dissertation. Swiss Federal Institute of Technology, Zurich, Switzerland, 1979.
25. Streeter, V.L., W.R. Keitzer, and D.F. Bohr. Pulsatile pressure and flow through distensible vessels. *Circ. Res.* 13:3, 1963.
26. Westerhof, N., F. Bosmann, C.J. DeVries, and A. Noordergraaf. Analog studies of the human systemic arterial tree. *J. Biomech.* 2:121–143, 1969.
27. Wetterer, E. and Th. Kenner. *Dynamik des Arterienpulses*. Springer, 1968.
28. Witzig, K. Ueber die Wellenbewegung zäher Flüssigkeiten in elastischen Röhren. Dissertation. University of Bern, 1914.
29. Womersley, J.R. An elastic tube theory of pulse transmission and oscillatory flow in mammalian arteries. WADC Tech. Rep. TR 56–614, 1957.
30. Zielke, W. Frequency-dependent friction in transient pipe flow. *ASME J. Basic Eng.* 90:Series D, No. 1, 109, 1968.